Biochimica et Biophysica Acta 1823 (2012) 2136–2148

Contents lists available at SciVerse ScienceDirect

Biochimica et Biophysica Acta

journal homepage: www.elsevier.com/locate/bbamcr

Distinctive roles of PLD signaling elicited by oxidative stress in synaptic endings from adult and aged rats

Melina V. Mateos, Norma M. Giusto, Gabriela A. Salvador *

Instituto de Investigaciones Bioquímicas de Bahía Blanca, Universidad Nacional del Sur and Consejo Nacional de Investigaciones Científicas y Técnicas, 8000 Bahía Blanca, Argentina

ARTICLE INFO

Article history:
Received 16 April 2012
Received in revised form 17 August 2012
Accepted 18 September 2012
Available online 23 September 2012

Keywords:
Phospholipase D
Protein kinase D
Oxidative injury
Aging
Diacylglycerol
Membrane microdomain

ABSTRACT

The role of iron in oxidative injury in the nervous system has been extensively described. However, little is known about the role of lipid signal transduction in neurodegeneration processes triggered by iron overload. The purpose of this work was to characterize the regulation and the crosstalk between phosphatidylcholine (PC)-derived diacylglycerol (DAG) and cannonical signaling pathways during iron-induced oxidative stress in cerebral cortex synaptic endings (Syn) obtained from adult (4 months old) and aged (28 months old) rats. DAG production was increased in Syn exposed to iron. This rise in DAG formation was due to phospholipase D1 (PLD1) and PLD2 activations. In adult rats, PKD1, ERK1/2 and PKCα/βII activations were PLD1 and PLD2 dependent. In contrast, in senile rats, DAG formation catalyzed by PLDs did not participate in PKD1, ERK1/2 and PKCα/βII regulations, but it was dependent on ERK and PKC activities. Iron-induced oxidative stress promoted an increased localization of PLD1 in membrane rafts, whereas PLD2 was excluded from these domains and appeared to be involved in glutamate transporter function. Our results show a differential regulation and synaptic function of DAG generated by PLDs during iron-induced oxidative stress as a consequence of aging.

1. Introduction

Phosphatidylcholine (PC) is the most abundant class of glycerophospholipids in mammalian cell membranes and it plays a key role in membrane structure, cell death, and cellular signaling. In regard to signal transduction, PC is the main substrate for phospholipase D (PLD), yielding phosphatidic acid (PA) and choline upon cleavage [1,2]. PA generated by PLD can be further hydrolyzed by lipid phosphate phosphatases (LPPs) in order to generate another lipid second messenger, diacylglycerol (DAG).

To date, two isoforms of mammalian PC-specific PLD (PLD1 and PLD2) have been cloned [3–5]. They share about 50% amino acid similarity, but exhibit quite different regulatory properties. PLD1 (120 kDa) has a low basal activity and responds to protein kinase C (PKC) and to members of the Rho and ARF families of small G proteins. PLD2, in contrast, exhibits a higher basal activity and presents a molecular weight of 100 kDa [1,2,6]. Involvement of PLD pathway has been proposed in several cellular events such as cytoskeletal rearrangement, vesicle trafficking, exocytosis, phagocytosis, oncogenesis, and neuronal and cardiac stimulation [6]. In the nervous system, PLD isoforms are present in neurons (independent of their transmitter) as well as in glial cells (astrocytes and oligondendrocytes) where they contribute to specific functions in e.g. cellular proliferation, exo- and endocytosis and neurite formation [6].

In healthy brains, iron levels are strictly maintained through highly regulated mechanisms of uptake, storage, and secretion. The ability of non-chelatable iron to accept and donate electrons leads to the formation of reactive nitrogen and oxygen species (RNS and ROS, respectively). These reactive species may trigger the oxidative attack of tissue components, causing brain lipid peroxidation, protein and DNA oxidation, impairment of membrane ion-motive ATPases, glucose and glutamate transport and mitochondrial function, thus contributing to disease and perhaps aging itself [7–9]. In neurons, synapses are sites where the first manifestations of neurodegenerative processes are likely to appear, and their vulnerability to iron-induced oxidative stress has been largely demonstrated by the presence of membrane lipid peroxidation, impairment of glucose and glutamate transport, and mitochondrial function [7,10–12]. The accumulation of transition metals (like iron) in the nervous system is a common observation in different neurodegenerative diseases, such as Parkinson's disease (PD), Alzheimer's disease (AD), Huntington's disease (HD) as well as amyotrophic lateral sclerosis (ALS) [13–15]. A large number of studies have demonstrated that metal-induced oxidative stress is one common feature in the onset of these neurodegenerative diseases [8,14].

Though a number of reports have described the intracellular events triggered by oxidative stress, very little is known about the role of lipid signal transduction during oxidative injury [16]. In line

* Corresponding author at: Instituto de Investigaciones Bioquímicas de Bahía Blanca, Centro Científico y Tecnológico CONICET Bahía Blanca and Universidad Nacional del Sur, Edificio E1, Camino La Carrindanga km 7, 8000 Bahía Blanca, Argentina. Tel.: +54 291 4861201; fax: +54 291 4861200.
E-mail address: salvador@criba.edu.ar (G.A. Salvador).

0167-4889/$ – see front matter © 2012 Elsevier B.V. All rights reserved.
http://dx.doi.org/10.1016/j.bbamcr.2012.09.005

with this, the participation of PLD in oxidative signaling has been described in cardiomyocites and PC12 cells [17,18]. Previous studies from our lab concluded that oxidative stress triggered by free iron enhances DAG generation from PC in synaptic endings (Syn) isolated from the cerebral cortex of adult and aged rats, and that this generation is in part due to the activation of PLD/LPP pathway [11]. We also demonstrated that both isoforms (PLD1 and PLD2) are present in Syn from adult and aged rats [19].

In view of the above, the aim of the present work is to address the role of PLD1 and PLD2 in synaptic DAG formation and in the activation of signal transduction pathways elicited by iron-induced oxidative stress, such as protein kinase D (PKD1), PKC and extracellular signal-regulated kinase (ERK) pathways. Furthermore, we explored the status of these signaling pathways in Syn obtained from aged animals.

2. Materials and methods

Wistar-INIBIBB strain adult (4 months old) and aged (24–28 months old) rats were kept under constant environmental conditions (24 °C and 12 h–12 h light–dark cycles) and fed on a standard pellet diet ad libitum. All proceedings were in accordance with *Principles of Use of Animals* and *Guide for the Care and Use of Laboratory Animals* (NIH regulation). Rats (males and females) were killed by using a CO_2 chamber. After death, rats were decapitated and cerebral cortices were immediately dissected (1–2 min after death) at 4 °C.

1-[^{14}C]palmitoyl-2-[^{14}C]palmitoyl-*sn*-glycero-3-phosphocholine ([^{14}C]-DPPC) (111 mCi/mmol), aminobutyric acid γ-[1-^{14}C] ([^{14}C]-GABA) (49.41 mCi/mmol) and glutamic acid, L-[3,4-^{3}H] ([^{3}H]-glutamate) (49,6 Ci/mmol) were purchased from New England Nuclear-Dupont, Boston, MA, USA. Preblended dry fluor 2a70 (98% PPO and 2% bis-MSB) was obtained from Research Products International Corp. (Mount Prospect, IL, USA). Triton X-100 (octyl phenoxy polyethoxyethanol), dimethyl sulfoxide (DMSO), 1,4-diamino-2,3-dicyano-1,4-bis[2-aminophenylthio]butadiene (U0126), Bisindolylmaleimide I (BIM), Chelerythrine chloride, Staurosporine, Phorbol 12-myristate 13-acetate (PMA) and thiobarbituric acid (TBA) were obtained from Sigma-Aldrich (St. Louis, MO, USA). (1R,2R)-N-([S]-1-{4-[5-bromo-2-oxo-2,3-dihydro-1H-benzo(d)imidazol-1-yl]piperidin-1-yl}propan-2-yl)-2-phenylcyclopropanecarboxamide (VU0359595 or EVJ), N-{2-[4-oxo-1-phenyl-1,3,8-triazaspiro(4.5) decan-8-yl]ethyl}quinoline-3-carboxamide (VU0285655-1 or APV) and 1,2-dioctanoyl-sn-glycerol (DOG) were from Avanti Polar Lipids, Inc. (Alabaster, AL, USA). The kit (Colestat enzimático AA) for measuring cholesterol was from Wiener laboratory (Rosario, Argentina). The kit for measuring protein content (DC protein assay) was from Bio-Rad Life Science group. Rabbit polyclonal antibodies anti-PKD1 (#2052), anti-Phospho-PKD1 (Ser744/728) (#2054), anti-ERK1/2 (#9102), anti-Phospho-ERK1/2 (#9101), anti-Phospho-PKCα/βII (Thr638/641) (#9375), anti-Phospho-PKCδ (Thr505) (#9374) and anti-PLD1 (#3832) were from Cell Signaling (Beverly, MA, USA). Mouse monoclonal anti-PKCα (#610107) and anti-PKCδ (#610397) were from BD Biosciences (San Jose, CA, USA). Rabbit polyclonal anti-Flotillin-1 antibody (sc-25506), goat polyclonal anti-PLD2 antibody (sc-48269), polyclonal horse radish peroxidase (HRP)-conjugated goat anti-rabbit IgG and polyclonal HRP-conjugated goat anti-mouse IgG were purchased from Santa Cruz Biotechnology, Inc. (Santa Cruz, CA, USA). All other chemicals were of the highest purity available.

2.1. Preparation of synaptosomal fraction

Total homogenates were prepared from the cerebral cortex (CC) of 4 month-old (adults) and 24–28 month-old (aged) rats. The same number of cortices from male and female rats was used in each experiment. Synaptosomes representing synaptic endings (Syn) were obtained as previously described by Cotman with slight modifications [19,20]. Briefly, CC homogenate (20%, w/v) was prepared in a medium containing 0.32 M sucrose, 1 mM EDTA, and 10 mM HEPES buffer (pH 7.4) in the presence of 1 mM DTT, 2 μg/ml leupeptin, 1 μg/ml aprotinin, 1 μg/ml pepstatin, and 0.1 mM PMSF. The CC was homogenized by 10 strokes with a Thomas tissue homogenizer. The homogenate was centrifuged at 1800 *g* for 7.5 min at 4 °C using a JA-21 rotor in a Beckman J2-21 centrifuge. The pellet was discarded and the supernatant was retained and centrifuged at 15,000 *g* for 20 min at 4 °C. The resulting pellet was washed and resuspended in 2 ml of 0.32 M sucrose isolation buffer, layered over a discontinuous Ficoll gradient (4 ml of 8.5% pH 7.4, 4 ml of 13% pH 7.4 Ficoll solutions, each prepared in isolation buffer) and spun at 100,000 *g* for 30 min at 4 °C using a SW 41 rotor in a Beckman Optima LK-90 ultracentrifuge. Syn in the 8.5%–13% Ficoll interface were removed, resuspended in isolation buffer, and centrifuged at 33,000 *g* for 20 min at 4 °C using a JA-21 rotor in a Beckman J2-21 centrifuge. For the experiments, synaptosomes were diluted in Tris base buffer medium (TBM) containing 120 mM NaCl, 5.0 mM KCl, 1.0 mM $MgCl_2$, 5 mM $NaHCO_3$, 1.2 mM Na_2HPO_4, 10 mM glucose, 20 mM Tris (pH 7.2), and protein content was determined by a previously published method [21] using the kit DC protein assay from Bio-Rad.

2.2. Experimental treatments

Syn were diluted in TBM, the suspension was aliquoted into tubes and incubated at 37 °C under an O_2:CO_2 (95:5, v/v) atmosphere during experimental treatments. Oxidative stress was induced by incubating Syn with 50 μM $FeSO_4$ for 1 or 2 h as previously described [11]. $FeSO_4$ was prepared as a 10 mM stock in ultrapure water immediately prior to use and the same volume of ultrapure water was added to the control condition.

To study the role of PLD isoforms, Syn were preincubated with 2% ethanol (EtOH), 0.15 μM EVJ (PLD1 inhibitor), 0.5 μM APV (PLD2 inhibitor) or Vehicle (DMSO 0.0025%) for 10 min at 37 °C before iron treatment. To study the role of PKC, Syn were preincubated with 1 μM PMA, 10 μM BIM, 0.1 μM Staurosporine, 5 μM Chelerythrine or vehicle (DMSO 0.0025%) for 10 min at 37 °C before iron treatment. To study the role of the MEK/ERK1/2 pathways, Syn were preincubated for 10 min at 37 °C in the presence of the MEK inhibitor U0126 (25 μM). To study the activation of ERK1/2 by exogenous DAG, Syn were treated with 0, 5 or 100 μM of DOG for 2 h at 37 °C.

2.3. Isolation of detergent-resistant membranes (DRMs)

DRMs were isolated from the entire Syn exposed to 50 μM $FeSO_4$ or to ultrapure water for 1 h. DRM fraction was isolated following the procedure previously described by Brown and Rose with slight modifications to our experimental system [19,22]. Briefly, the synaptosomal pellet obtained from 2 CC was resuspended in 1.6 ml of iced-cold (0–4 °C) lysis buffer consisting of 1% Triton X-100 in DRM buffer (10 mM Tris–HCl (pH 7.4), 70 mM NaCl, 2 mM $MgCl_2$ and 0.5 mM EDTA) with protease inhibitors added (1 mM DTT, 2 μg/ml leupeptin, 1 μg/ml aprotinin, 1 μg/ml pepstatin, and 0.1 mM PMSF). The suspension was homogenized by passing it through a 21 G×1 1/2″ needle 4–5 times and it was incubated at 4 °C for 30 min. The homogenization was repeated after 15 min of incubation. The homogenate was subsequently centrifuged at 1000 *g* for 15 min at 4 °C (2500 rpm, Beckman JA-21 rotor, Beckman J2-21 centrifuge). The supernatant was diluted 1:1 in 80% (w/v) sucrose, divided into two samples and placed at the bottom of ultracentrifuge tubes. Additionally, 6.6 ml of 30% (w/v) sucrose was layered, followed by 2.6 ml 5% (w/v) sucrose. All the sucrose solutions were handled at 0–4 °C and diluted in the DRM buffer (without Triton X-100) containing protease inhibitors (1 mM DTT, 2 μg/ml leupeptin, 1 μg/ml aprotinin, 1 μg/ml pepstatin, and 0.1 mM PMSF). Samples were centrifuged for 20 h at 120,000 *g* (Beckman SW 41 rotor in a Beckman Optima LK-90 ultracentrifuge) at 4 °C. After the

centrifugation three visible floating bands (DRMs, B2 and B3) and a pellet were obtained. The band containing the DRMs was present in the 5–30% sucrose interface. The fractions were collected and transferred to a new centrifuge tube, which was filled up with DRM buffer and centrifuged for 1 h at 120,000 *g* in a Beckman 90Ti rotor using a Beckman Optima LK-90 ultracentrifuge. The following pellets were resuspended in TBM buffer and protein content was determined by a previously published method [21] using the DC protein assay kit from Bio-Rad.

2.4. Determination of DAG generation from PC

PC hydrolysis was determined using lipid vesicles containing [^{14}C]-DPPC and cold DPPC to yield 45,000 dpm and 0.125 mM per assay in a buffer containing 0.2% Triton X-100 and 0.1 M Tris (pH 7.2). 100 μl of these lipid vesicles was added to 100 μl of treated Syn or DRMs (200 μg of protein) in a final volume of 200 μl. The reaction was carried out at 37 °C for 20 min and stopped by the addition of 5 ml of chloroform:methanol (2:1, v/v). Blanks were prepared identically, except that membranes were boiled for 5 min before use. Lipids were extracted and separated as described below [11,19]. To evaluate the contribution of PLD pathway to DAG formation, the enzyme reaction was carried out in the presence of 2% EtOH [11,19]. To evaluate the contribution of PLD1 and PLD2 isoforms, Syn were preincubated with their specific inhibitors (0.15 μM EVJ and 0.5 μM APV) as described above.

2.5. [^{14}C]-DAG isolation and quantification

After the enzyme reaction, lipids were extracted as previously described [11]. Briefly, the lipid extract was washed with 0.2 volumes of 0.05% $CaCl_2$ and the lower phase was obtained after centrifugation at 900 *g* for 5 min. Diacylglycerol (DAG) was then separated by one-dimensional thin-layer chromatography (TLC) using silica gel G plates (Merck) in a mobile phase consisting of hexane:diethyl ether: acetic acid (50:50:2.6, v/v). PC was retained at the spotting site. Lipids were visualized by exposure of the plate to iodine vapors and DAG spots were scraped off the plate and radioactivity was determined by liquid scintillation as previously described [11,19].

2.6. Lipid phosphorus measurement

In order to determine lipid phosphorus (lipid P), phospholipids (PLs) were visualized by exposure of the plate to iodine vapors and lipid P was determined in each spot (and previously in total lipid extracts) using the chemicals and reactions described by Rouser and collaborators [23].

2.7. Cholesterol measurement

Total cholesterol content was measured in aliquots of the lipid extracts corresponding to 5 μg lipid P, using a commercial kit (Colestat enzimático AA) from Wiener laboratory. The aliquots were dried under N_2 gas and resuspended in 100 μl of isopropyl alcohol, and the manufacturer's instructions were subsequently followed. Briefly, the method is based on a series of enzyme reactions: firstly, cholesterol esterase hydrolyzes cholesterol esters to cholesterol and free fatty acids (FFA), and secondly, cholesterol oxidase oxidizes cholesterol to cholesten-3-ona plus H_2O_2 which, in turn, reacts with 4-aminophenazone to generate a red compound (quinonimine) that can be measured spectrophotometrically at 505 nm [19].

2.8. Lipid peroxidation assay

Lipid peroxidation was measured using the thiobarbituric acid assay as previously described [11,24]. Briefly, after 1 h incubation in the presence of either Fe^{2+} or vehicle, 1 ml of 30% trichloroacetic acid (TCA) was added to 0.5 ml of Syn or DRMs (300 μg protein). Then, 0.1 ml of 5 N HCl and 1 ml of 0.75% thiobarbituric acid were added. Tubes were capped, the mixtures were heated at 100 °C for 15 min in a boiling water bath and the samples were centrifuged at 1000 *g* for 10 min. Thiobarbituric acid reactive substances (TBARS) were measured in the supernatant at 535 nm and results were expressed as units of absorbance at 535 nm per μmol of PLs (Abs 535 nm/μmol of PLs).

2.9. Sodium dodecyl sulfate-polyacrylamide gel electrophoresis (SDS-PAGE) and Western blot (WB) assays

Syn and DRMs samples were denatured with Laemmli sample buffer at 100 °C for 5 min [25]. Equivalent amounts of synaptosomal, DRM proteins and other fraction's proteins (30 μg) from adult and aged animals were separated by sodium dodecyl sulfate-polyacrylamide gel electrophoresis (SDS-PAGE) on 10% polyacrylamide gels and subsequently transferred to polyvinylidene fluoride (PVDF) membranes (Millipore, Bedford, MA, USA) which were blocked with 10% bovine serum albumin (BSA) in TTBS buffer [20 mM Tris–HCl (pH 7.4), 100 mM NaCl and 0.1% (w/v) Tween 20] at room temperature for 2 h. Membranes were subsequently incubated with primary antibodies [anti-Phospho-PKCα/βII (1:2000),

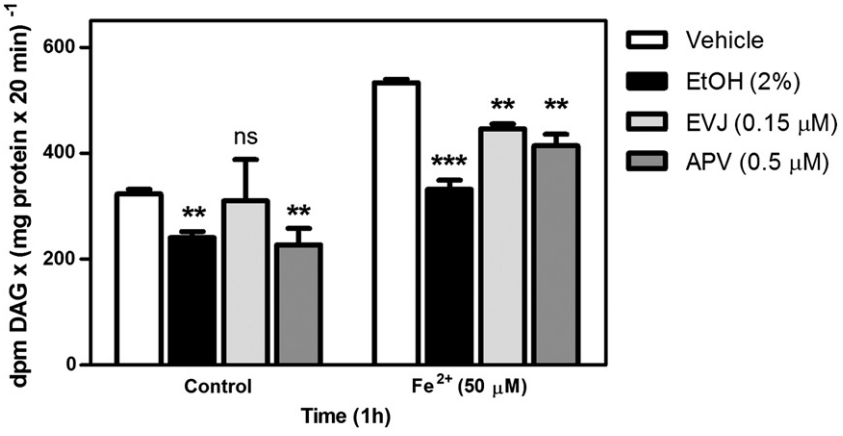

Fig. 1. PLD1 and PLD2 contributions to DAG generation elicited by iron-induced oxidative stress. CC Syn were isolated from adult rats and preincubated in TBM medium in the presence of the vehicle (DMSO), EVJ (0.15 μM) or APV (0.5 μM) at 37 °C for 10 min. After preincubation, Syn were treated with 50 μM $FeSO_4$ or ultrapure water (control condition) for 1 h. Enzyme reaction was started by adding 100 μl of preincubated Syn (200 μg protein) to 100 μl of lipid vesicles containing [^{14}C]-DPPC and non-radiolabeled DPPC to yield 45,000 dpm and 0.125 mM per assay, in the presence or in the absence of EtOH (2%). After 20 min incubation at 37 °C the enzyme reaction was stopped and lipids were extracted, isolated and [^{14}C]-DAG was separated and quantified as described in Materials and methods. Results are expressed as dpm [^{14}C]-DAG × (mg protein × 20 min)$^{-1}$. Asterisks indicate significant differences with respect to the vehicle condition (***$p<0.001$; **$p<0.01$).

anti-Phospho-PKCδ (1:2000), anti-Flotillin-1 (1:5000), anti-ERK1/2 (1:1000), anti-Phospho-ERK1/2 (1:1000), anti-PKCα (1:1000) and anti-PKCδ (1:1000) at room temperature for 2 h; anti-PLD1 (1:300), anti-PLD2 (1:300), anti-PKD1 (1:500) and anti-Phospho-PKD1 (1:500) overnight at 4 °C], washed three times with TTBS and then exposed to the appropriate HRP-conjugated secondary antibody (anti-rabbit or anti-mouse) for 2 h at room temperature. Membranes were washed again three times with TTBS and immunoreactive bands were detected by enhanced chemiluminescence (ECL, Amersham Biosciences) using standard X-ray film (Kodak X-Omat AR).

2.10. Glutamate and GABA uptake assays

For the glutamate and GABA uptake assays, Syn were preincubated with 0.15 μM EVJ, 0.5 μM APV, 10 μM BIM, 25 μM U0126 or Vehicle (DMSO 0.0025%) for 10 min at 37 °C. After preincubation, oxidative stress was induced by incubating Syn with 50 μM $FeSO_4$ on ultrapure water (control condition) for 1 h as previously described. Either 100 μl control or Fe^{2+}-treated Syn (200 μg protein) were incubated for 7 min at 37 °C with 100 μl of 4 mM $CaCl_2$ TBM containing [^{3}H]-glutamate or [^{14}C]-GABA (0.1 μCi/ml). The uptake reaction was stopped by dilution with 800 μl of iced-cold TBM. Syn were then pelleted, washed three times with 500 μl of iced-cold phosphate buffered saline (PBS) and lysed in 400 μl of solution of 5% sodium dodecyl sulfate (SDS) in PBS. The lysate was placed in scintillation vials and radioactivity was determined by liquid scintillation. Results were expressed as dpm/mg protein × min.

2.11. Statistical analysis

Statistical analysis was performed using ANOVA followed by Bonferroni's test to compare means. *p*-values lower than 0.05 were considered statistically significant. Data represent the mean value ± SD of three independent experiments using a pool of four animals on each occasion. The WBs shown are representative of three analyses carried out on samples from three independent experiments.

3. Results

3.1. PLD1 and PLD2 contributions to DAG generation elicited by iron-induced oxidative stress

We have previously demonstrated that rat CC Syn incubated with $FeSO_4$ (50 μM) constitute an appropriate model for studying the effect of oxidative damage on synaptic endings [11,12]. In Syn exposed to Fe^{2+} there was an increase in lipid peroxidation [measured as thiobarbituric acid reactive substances (TBARS) formation], a reduced glutamate uptake and mitochondrial function (measured as MTT reduction) and the plasma membrane integrity was also affected (evaluated as LDH leakage to the external medium) [11,12]. We have also demonstrated that iron-induced oxidative stress stimulates DAG generation from PC in Syn from adult and aged rats due to the activation of PC-specific phospholipase C (PC-PLC) and PLD/LPP pathways [11]. In the present work we further study the role of PLD1 and PLD2 isoforms in DAG formation and their participation in the activation of PKD1, PKC and ERK pathways under iron-induced oxidative stress.

To study the particular role of PLD1 and PLD2, two recently developed isoform-specific inhibitors were used. Syn from adult rats were preincubated with 0.15 μM EVJ (PLD1 inhibitor), 0.5 μM APV (PLD2 inhibitor) or vehicle (DMSO, 0.0025% final concentration) for 10 min at 37 °C before treatment with iron or the same volume of ultrapure H_2O (control condition) for 1 h as described in Materials and methods. To further analyze the contribution of PLD pathway to DAG formation, the enzyme reaction was also carried out in the presence of 2% ethanol (EtOH). EtOH was added in order to avoid DAG generation because in the presence of primary alcohols, PLDs exclusively catalyze a transphosphatidylation reaction yielding phosphatidylalcohols instead of PA. Thus, phosphatidylalcohol generation blocks LPP action and prevents DAG formation from occurring via PLD/LPP pathway [11,19]. After the treatment, [^{14}C]-DAG formation from [^{14}C]-DPPC was measured as described in Materials and methods. Fig. 1 shows that under the control condition [^{14}C]-DAG formation was partially reduced to similar levels by EtOH and the PLD2 inhibitor, APV (25 and 30%, respectively). Iron treatment for 1h increased [^{14}C]-DAG by 65% and this rise was partially reduced by the preincubation with EVJ and APV (16% and 23% respectively). Interestingly, the sum of the effect of PLD1 and PLD2 inhibitors is in agreement with the reduction of DAG formation observed in the presence of 2% EtOH (38%). These results indicate that under the control condition only PLD2 is constitutively active in the synaptic ending whereas both PLDs contribute to DAG formation under oxidative injury conditions.

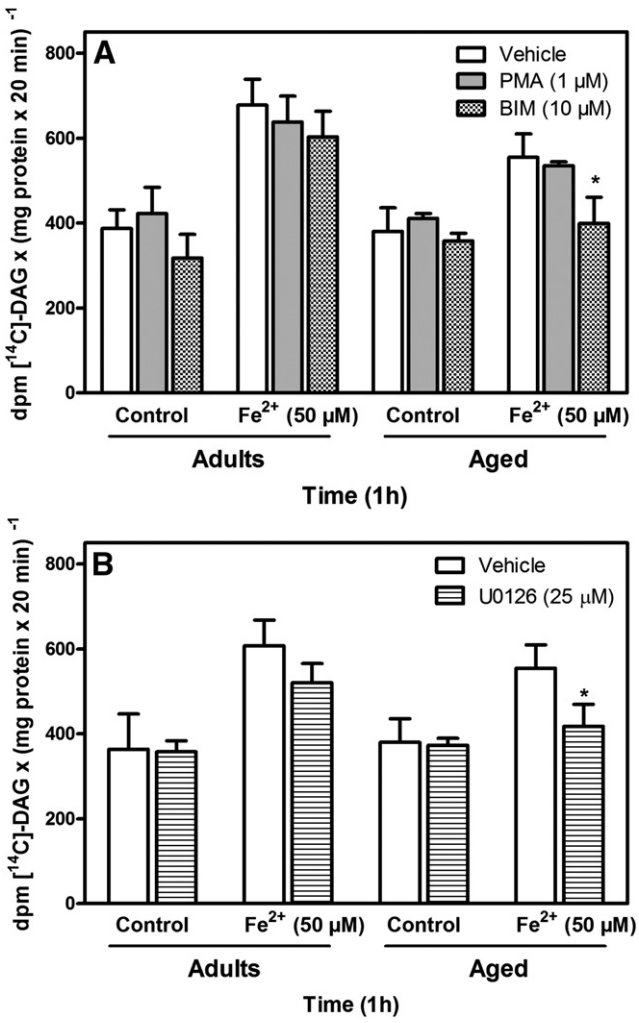

Fig. 2. Modulation of DAG formation by PKC and MEK/ERK pathways during iron-induced oxidative stress. A) Modulation of DAG formation by PKC. Syn from adult and aged rats were preincubated in TBM in the presence of vehicle (DMSO), PMA (1 μM) or BIM (10 μM) for 10 min at 37 °C. After preincubation, Syn were treated with 50 μM $FeSO_4$ or ultrapure water (control condition) for 1 h. B) Modulation of DAG formation by MEK/ERK pathway. Syn from adult and aged rats were preincubated in TBM in the presence of vehicle (DMSO) or U0126 (25 μM) at 37 °C for 10 min. After preincubation, Syn were treated with 50 μM $FeSO_4$ or H_2O (control condition) for 1 h. For A and B the enzyme reaction and [^{14}C]-DAG isolation and quantification were performed as described in Fig. 1. Results are expressed as dpm [^{14}C]-DAG × (mg protein × 20 min)$^{-1}$. Asterisks indicate significant differences with respect to the vehicle condition (*p<0.05).

3.2. Modulation of DAG formation by PKC and MEK/ERK pathways during iron-induced oxidative stress

To study the role of PKC on DAG generation during synaptic oxidative injury, Syn from adult and aged rats were preincubated with phorbol ester PMA (1 μM) or with PKC inhibitor BIM (10 μM). After preincubation, Syn were treated with either $FeSO_4$ (50 μM) or ultrapure water (control condition) for 1 h. In Syn from adult rats neither PKC activation by PMA nor PKC inhibition affected DAG formation (Fig. 2A). In contrast, the presence of BIM completely abolished the increase in DAG levels induced by iron in aged animals while preincubation with PMA had no effect on DAG levels (Fig. 2A). Our results suggest a differential regulation of PLD pathways during iron-induced oxidative injury in adult and aged animals. Syn from adult rats were also preincubated with two different PKC inhibitors Staurosporine (0.1 μM) and Chelerythrine (5 μM) neither of which affected DAG levels (data not shown).

To further characterize the signaling pathways involved in DAG generation, Syn were preincubated with the MEK inhibitor U0126 (25 μM), which is the immediate upstream regulator of ERK1/2. As shown in Fig. 2B, while MEK kinase inhibition was observed not to affect DAG formation from PC in Syn isolated from adult rats it abolished the increase in DAG levels induced by iron in Syn from aged rats (Fig. 2B). These results suggest that only in Syn from aged animals the activation of DAG generating enzymes by oxidative stress depends on the activation of MEK/ERK1/2 pathway.

3.3. Activation of PKD1, PKCα/βII, PKCδ and ERK1/2 by synaptic iron-induced oxidative stress

In view of the rise in DAG levels generated by iron-induced oxidative stress, we next studied the activation of several DAG responding proteins, namely PKD1, PKCα/βII and PKCδ. Moreover, since the activation of RasGRP by DAG leads to the activation of the Ras/MEK/ERK pathway, we also studied the activation of ERK1/2. To study the activation of these signaling pathways, Western blot (WB) assays were performed using primary antibodies raised against the phosphorylated active forms of PKD1, PKCα/βII, PKCδ and ERK1/2. Fig. 3 shows that in adult rats 2 h iron treatment strongly activates PKD1 and ERK1/2 with respect to the control condition (120 and 600%, respectively). PKCα/βII (conventional PKCs) and PKCδ (novel PKC) were also activated by oxidative stress (60 and 50%, respectively). Loading controls were performed by detecting total PKD1, ERK1/2, PKCα and PKCδ (Fig. 3). After 1 h of treatment with 50 μM $FeSO_4$ ERK1/2 activation was 45% higher with respect to the control whereas no increase in PKD1 phosphorylation was detected (data not shown).

3.4. Role of PLD isoforms and PKC on PKD1, PKCα/βII and ERK1/2 activation during iron induced oxidative stress

To study the participation of PLD1, PLD2 and PKCs in the activation of PKD1, PKCα/βII and ERK1/2, Syn from adult and aged rats were preincubated in the presence of EtOH (2%), PLD1 inhibitor EVJ (0.15 μM), PLD2 inhibitor APV (0.5 μM) or PKC inhibitor BIM (10 μM).

In Syn from adult rats, EtOH, EVJ, APV and BIM strongly reduced ERK1/2 activation elicited by iron-induced oxidative stress (1 h treatment with $FeSO_4$) (Fig. 4A, first panel). The increase in PKCα/βII phosphorylation after 1 h exposure to iron was also reduced by the preincubation with EtOH, EVJ, APV and BIM (Fig. 4A, second panel). The effect of these inhibitors on PKD1 phosphorylation was only studied after 2 h of oxidative insult on account of the fact that its activation was observed at this time (data not shown). After 2 h treatment with $FeSO_4$ ERK1/2, PKD1 and PKCα/βII activations was also reduced by EtOH, EVJ, APV and BIM (Fig. 4B). In line with this,

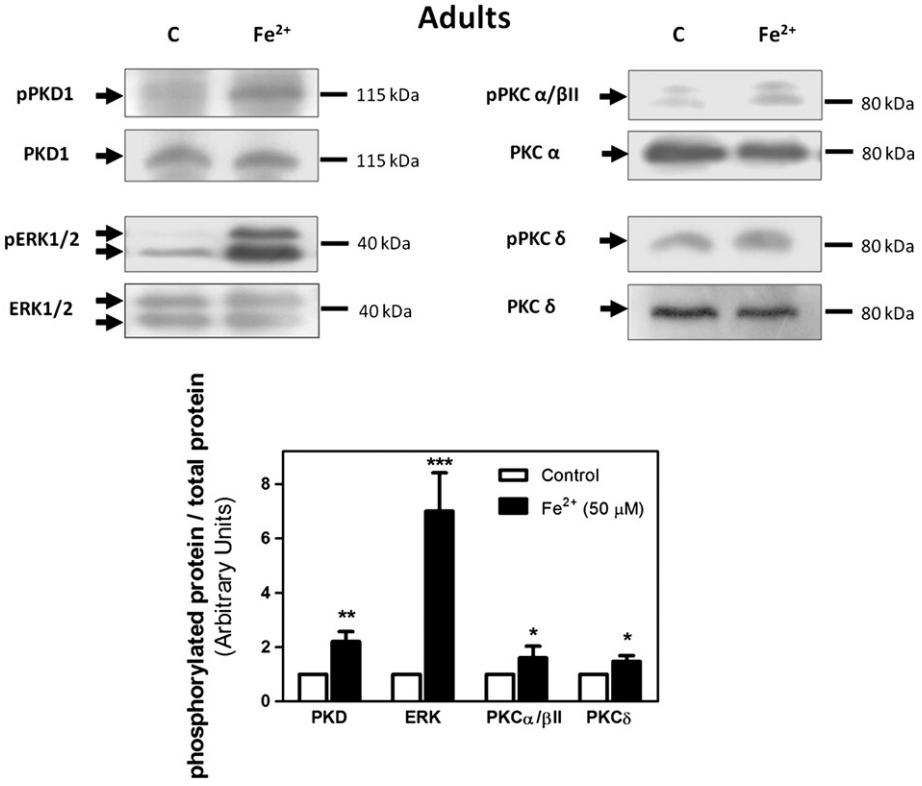

Fig. 3. Activation of PKD1, PKCα/βII, PKCδ and ERK1/2 by $FeSO_4$ exposure. CC Syn from adult rats were treated with 50 μM $FeSO_4$ (Fe^{2+}) or ultrapure water (control condition, C) for 2 h. For Western Blot (WB) assays Syn proteins (30 μg) were resolved in a 10% SDS-PAGE and transferred to a PDVF membrane. Membranes were blocked, incubated with primary and secondary antibodies as detailed in Materials and methods. Immunoreactive bands were detected by enhanced chemiluminescence. Numbers to the right indicate molecular weights and data shown is a representative result of three independent experiments. The bar graph shows the densitometry values of phosphorylated protein/non phosphorylated protein expressed as ratio of control. Asterisks indicate significant differences with respect to the control condition (***$p<0.001$; **$p<0.01$; *$p<0.05$).

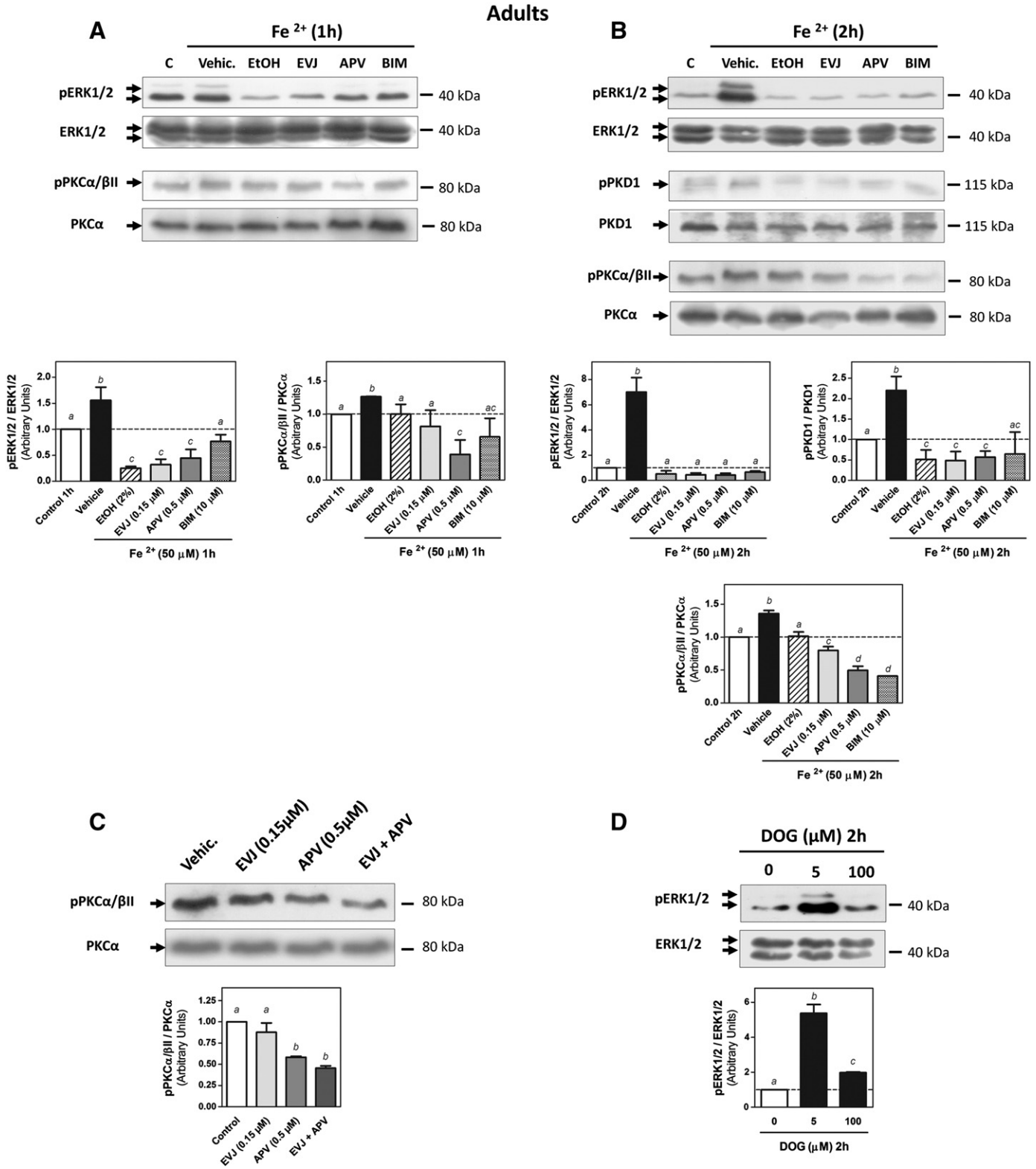

Fig. 4. Role of PLD isoforms and PKC on PKD1, PKCα/βII and ERK1/2 activations during iron-induced oxidative stress in Syn from adult rats. CC Syn from adult rats were preincubated in the presence of vehicle (DMSO), ethanol (2%), EVJ (0.15 μM), APV (0.5 μM) or BIM (10 μM) at 37 °C for 10 min. After preincubation, Syn were treated with 50 μM $FeSO_4$ (Fe^{2+}) or ultrapure water (control condition, C) for 1 (A) or 2 h (B). C) Effect of PLD inhibitors on PKC activation. CC Syn from adult rats were preincubated in the presence of vehicle (DMSO), EVJ (0.15 μM), APV (0.5 μM) or EVJ plus APV for 10 min at 37 °C. D) ERK1/2 activation by exogenous DAG. CC Syn from adult rats were treated with 0, 5 or 100 μM of DOG for 2 h as described in Materials and methods. For A–D WB assays were performed as described in Fig. 3. Numbers to the right indicate molecular weights and data shown is a representative result of three independent experiments. The bar graphs show the densitometry values of phosphorylated protein/non-phosphorylated protein expressed as ratio of control. (a–d) indicate significant differences ($p<0.05$).

ERK1/2 activation was also induced by 2 h treatment with 5 μM (similar to DAG levels generated under synaptosomal PLD activation conditions) and 100 μM 1,2-dioctanoyl-sn-glycerol (DOG), 430 and 97% respectively (Fig. 4D). In addition, PKCα/βII activation was also dependent on PLD1 and PLD2 activities and the inhibition of classical PKCs was observed to avoid ERK and PKD1 activation. These results suggest that in adult Syn exposed to oxidative injury PLD1 and PLD2 are upstream effectors for ERK and PKD1 activation.

Under control conditions, PKCα/βII phosphorylation was partially reduced by PLD2 inhibitor APV but was not affected by PLD1 inhibitor EVJ (Fig. 4C). This is consistent with the decrease in DAG levels observed under control conditions in the presence of APV, thus being indicative of the presence of a constitutive activity of PLD2 (Fig. 1).

In contrast, in Syn from aged rats the presence of EtOH, EVJ, APV and BIM did not prevent ERK1/2, PKD1 and PKCα/βII activations induced by 1 h treatment with $FeSO_4$ (Fig. 5A) from occurring. After 2 h of treatment with iron, ERK1/2 activation was reduced to control levels by the preincubation with EtOH and PLD2 inhibitor APV and was also partially reduced by BIM while it was not affected by PLD1 inhibitor EVJ (Fig. 5B). In Syn isolated from aged rats, PKD1 activation was observed earlier than in adults (after 1 h of treatment with $FeSO_4$) and after 2 h of oxidative injury PKD1 phosphorylation was reduced with respect to the control condition (Fig. 5A and B, second panels). Moreover, in Syn from aged animals exposed to oxidative damage for 2 h no differences in PKCα/βII phosphorylation were detected between the different experimental conditions and the control condition (Fig. 5B). These results demonstrate that the regulation and time course activation of PKD1, PKCα/βII and ERK1/2 pathways in synaptic endings from aged animals differ completely from those observed in adults. After 1 h of treatment with iron ERK and PKD, activation was not dependent on PLD or PKC activities while after 2 h of treatment ERK activation seemed to be PLD2 and PKC dependent while it was not affected by PLD1 inhibition. After the 2 h incubation period, no PKCα/βII activation was observed in aged rats whereas PKD1 activation was found to decrease compared to the control condition.

3.5. Effect of iron-induced oxidative stress on glutamate and GABA uptake assays

Previous studies have characterized the impairment of glutamate and gamma aminobutyric acid (GABA) transport after the exposure of synaptosomes to oxidative insults [10,12,26,27]. Under our

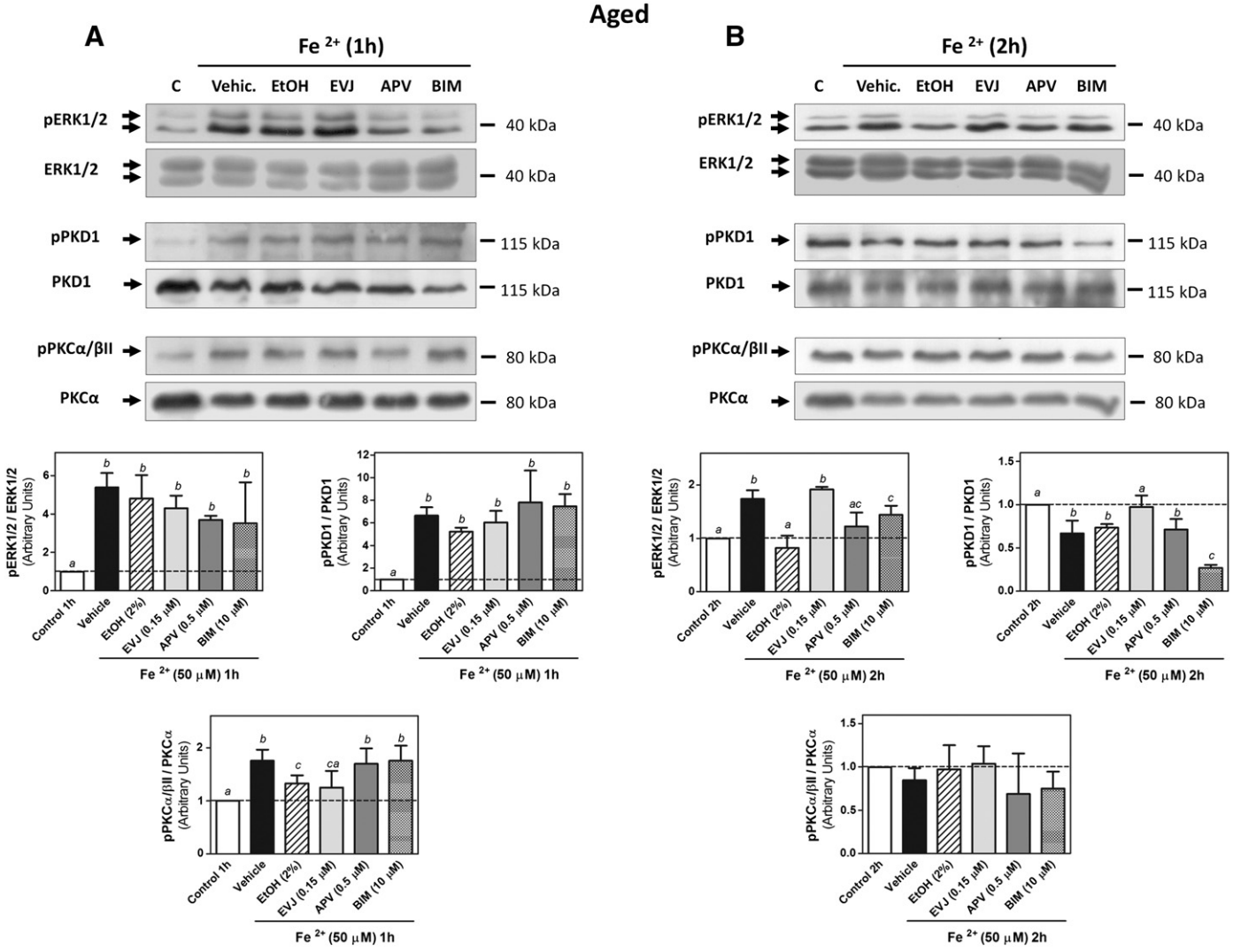

Fig. 5. Role of PLD isoforms and PKC on PKD1, PKCα/βII and ERK1/2 activations during iron-induced oxidative stress in Syn from aged rats. CC Syn from aged rats were preincubated in the presence of vehicle (DMSO), ethanol (2%), EVJ (0.15 μM), APV (0.5 μM) or BIM (10 μM) at 37 °C for 10 min. After preincubation, Syn were treated with 50 μM $FeSO_4$ (Fe^{2+}) or ultrapure water (control condition, C) for 1 (A) or 2 h (B) and WB assays were performed as described in Fig. 3. Numbers to the right indicate molecular weights and data shown is a representative result of three independent experiments. The bar graphs show the densitometry values of phosphorylated protein/total protein expressed as ratio of control. (a–d) indicate significant differences ($p<0.05$).

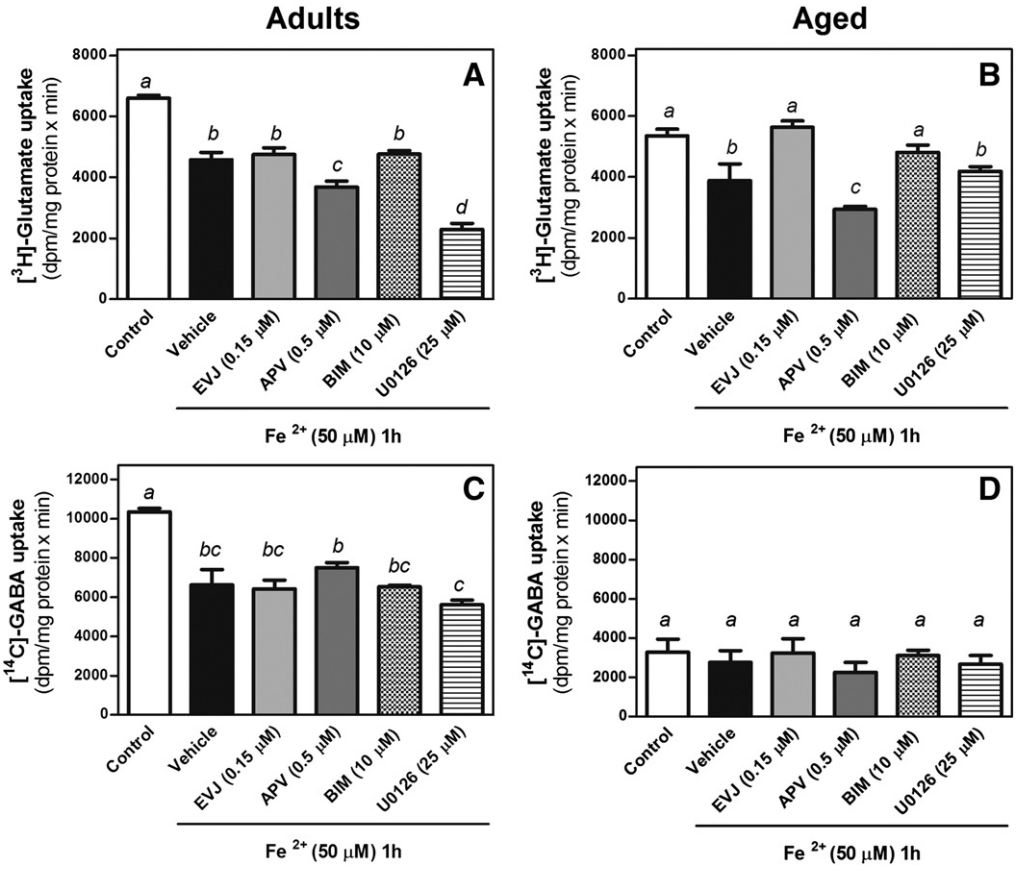

Fig. 6. Effect of iron-induced oxidative stress on glutamate and GABA uptake assays. CC Syn from adult and aged rats were preincubated in the presence of vehicle (DMSO), EVJ (0.15 μM), APV (0.5 μM), BIM (10 μM) or U0126 (25 μM) at 37 °C for 10 min. After preincubation, Syn were treated with 50 μM $FeSO_4$ or H_2O (control condition) for 1 h. Uptakes were started by adding 100 μl of preincubated synaptosomal suspensions (200 μg protein) to 100 μl of buffer containing 0.1 μCi of [^{3}H]-glutamate or [^{14}C]-GABA per assay. After 7 min of incubation at 37 °C the uptakes were stopped by dilution in cold buffer and washed as described in Materials and methods. A) [^{3}H]-glutamate uptake in Syn from adult rats. B) [^{3}H]-glutamate uptake in Syn from aged rats. C) [^{14}C]-GABA uptake in Syn from adult rats. D) [^{14}C]-GABA uptake in Syn from aged rats. Results are expressed as dpm/mg protein × min. (a–d) indicate significant differences ($p<0.05$).

experimental conditions [^{3}H]-glutamate and [^{14}C]-GABA uptakes were significantly reduced in adult Syn exposed for 1 h to $FeSO_4$ (31% and 36%, respectively; Fig. 6A and C). Preincubation with PLD1 inhibitor EVJ (0.15 μM) or with PKC inhibitor BIM (10 μM) did not affect [^{3}H]-glutamate uptake with respect to the vehicle condition. However, preincubation with PLD2 inhibitor APV (0.5 μM) or with MEK inhibitor U0126 (25 μM) reduced even more the uptake of [^{3}H]-glutamate (45% and 65%, respectively; Fig. 6A). In a different way, PLD1, PLD2, PKC and MEK inhibitions did not affect the impairment in GABA transport induced by iron treatment (Fig. 6C). These results suggest that in Syn from adult animals PLD2 and MEK/ERK pathways participate in the protection against the deleterious effect of iron on the glutamate transporter (GLT). In contrast, none of the signaling pathways studied (PLD1, PLD2, PKC and MEK/ERK) seemed to be involved in the impairment of GABA uptake induced by the oxidative injury.

Fig. 6B shows that in Syn from aged rats iron treatment also reduced [^{3}H]-glutamate uptake with respect to the control condition (28%) and preincubation with PLD2 inhibitor APV (0.5 μM) reduced even more the uptake of the neurotransmitter (45%). However, PLD1 and PKC inhibition restored [^{3}H]-glutamate uptake to the levels observed under the control condition while MEK inhibition did not modify impairment in glutamate uptake induced by oxidative stress (Fig. 6B). These results suggest that also in Syn from aged animals PLD2 protects GLT against the deleterious effect of iron whereas PLD1 and some PKC isoforms produce a deleterious effect on the neurotransmitter uptake. Our results also show that GABA uptake is severely reduced in Syn from aged animals with respect to adults (68%, Fig. 6D). In addition, in Syn from aged rats GABA transporter (GAT) was neither affected by oxidative damage nor modulated by the signaling pathways studied (Fig. 6D).

3.6. DAG generation from PC in detergent resistant membranes (DRMs) during iron-induced oxidative stress

Membrane rafts are small (10–200 nm), heterogeneous, sterol- and sphingolipid-enriched domains that compartmentalize important cellular processes such as cell adhesion and endocytosis and they have been proposed as signal transduction platforms and as key regulators of several signaling pathways [28,29]. One of the first methods originally used for the study of these domains was based on their insolubility in non-ionic detergent such as Triton X-100 [22].

We have previously reported that the detergent resistant membrane (DRM) fraction obtained from CC Syn evidenced typical characteristics of membrane rafts, e.g. high content of sphingomyelin and cholesterol and enrichment in caveolin, c-Src and flotillin-1, three proteins widely used as markers of membrane rafts. The DRM fraction showed a more saturated fatty acid composition than synaptosomes, with a great decrease in the content of polyunsaturated fatty acids (PUFA) 20:4n-6 and 22:6n-3 (80%) and an enrichment in 16:0 (34%). Moreover, compared to adults, Syn and DRMs from aged animals also revealed a dramatic decrease in the fatty acids 20:4n-6 and 22:6n-3 [19]. We also demonstrated a differential localization of PC-PLC and PLD isoforms in DRMs and entire Syn, i.e. whereas PLD1 and PC-PLC were concentrated in DRMs, PLD2 was excluded from this fraction. Interestingly, in the DRM fraction DAG formation did not decrease in the presence of EtOH, thus indicating that no PLD

activity was detected in DRMs even though PLD1 was concentrated in this fraction [19].

To further study the effect of iron-induced oxidative stress on DAG generating pathways, PLD1 and PLD2 localizations in the DRM fraction as well as their distribution in the fractions isolated from the sucrose gradient were studied as a function of oxidative stress.

To assess these two items, DRMs were isolated from entire Syn exposed to 50 μM $FeSO_4$ or to the control condition for 1 or 2 h as described in Materials and methods. The isolation of the DRM fraction was based on their detergent insolubility at low temperature and low buoyant density upon discontinuous sucrose density gradient centrifugation. After a 20 h centrifugation at 120,000 *g*, three visible floating bands (DRMs, B2 and B3) and a pellet were obtained. The band containing DRMs was present in the 5–30% sucrose interface (see schema in Fig. 8A) and [^{14}C]-DAG generation from [^{14}C]-DPPC was measured as detailed in Materials and methods, either in the presence of EtOH (2%) or the vehicle.

Fig. 7A shows that, in contrast to the results obtained in entire Syn, in the DRM fraction from adult rats [^{14}C]-DAG generation from [^{14}C]-DPPC was not increased after 1 or 2 h treatment with $FeSO_4$. Likewise, no differences were observed in the presence of 2% EtOH (Fig. 7A). These results indicate that DAG generation in the membrane raft fraction is not affected by oxidative stress in spite of the enrichment in PLD1 and PC-PLC isoforms previously reported in these microdomains [19].

Lipid peroxidation (measured as TBARS formation) was greatly increased in Syn from adult and aged rats exposed for 1 h to $FeSO_4$ (370 and 770% with respect to the control condition) (Fig. 7B). However, DRM fractions isolated from adult and aged rats showed no increase in lipid peroxidation after iron-induced oxidative stress (Fig. 7B). These results are in accordance with the more saturated fatty acid composition previously reported for the membrane raft fraction [19]. On the other hand, lipid peroxidation levels in both fractions isolated from aged animals (Syn and DRM) were lower than those observed in adult animals, which is also in agreement with the decrease in PUFA previously reported in aged animals compared to adults [19].

As described above, three floating bands (DRMs, B2 and B3) and a pellet were obtained from adult Syn exposed to $FeSO_4$ or to the control condition for 1 h (see schema in Fig. 8A). The protein content of each fraction was determined and equivalent amounts of proteins (30 μg) were resolved by SDS-PAGE. The presence of PLD1, PLD2 and Flotillin-1 in the different fractions was determined by WB as described in Materials and methods.

PLD1 and Flotillin-1 were enriched in DRMs and in the second floating band (B2) while PLD2 was enriched in the pellet and was completely excluded from the floating bands (DRMs, B2 and B3). Iron treatment induced an enhanced localization of PLD1 in DRMs and in B2 whereas Flotillin-1 localization in DRMs was decreased. Furthermore, PLD2 distribution was not affected by iron treatment (Fig. 8A) while $FeSO_4$ exposure induced no changes in the total protein distribution among the sucrose gradient nor in the cholesterol content of Syn and DRMs (Fig. 8B and C, respectively).

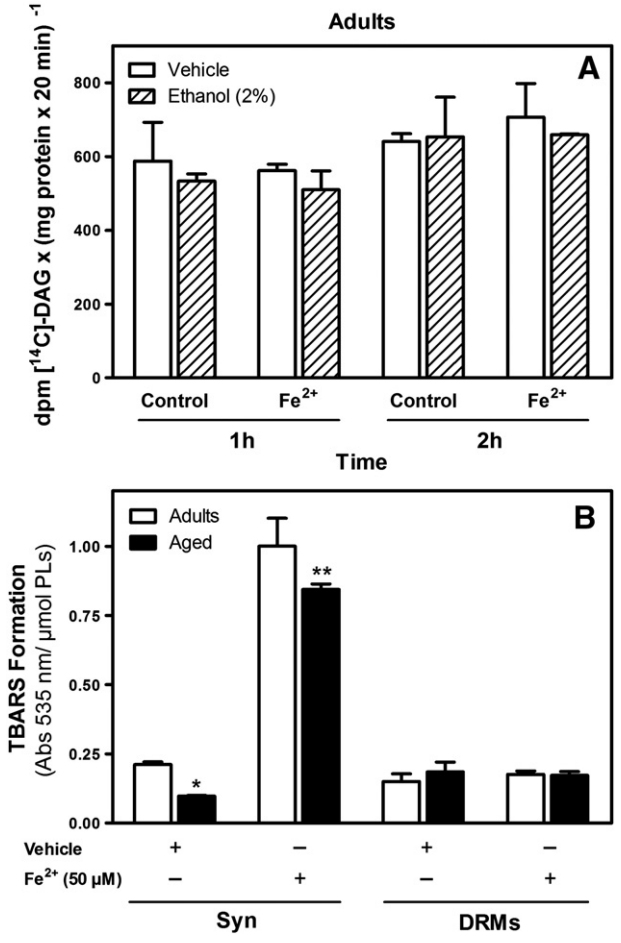

Fig. 7. DAG generation from PC in detergent resistant membranes (DRMs) during iron-induced oxidative stress. A) DAG generation from PC in DRMs exposed to $FeSO_4$. DRMs were isolated by their relative insolubility in cold Triton X-100 from CC Syn from adult rats exposed to 50 μM $FeSO_4$ or to the control condition (ultrapure water) for 1 or 2 h. After treatment, the enzyme reaction was performed in the presence of ethanol (2%) or vehicle (ultrapure water) as described in Fig. 1. [^{14}C]-DAG isolation and quantification were performed as described in Fig. 1. Results are expressed as dpm [^{14}C]-DAG × (mg protein × 20 min)$^{-1}$. B) Lipid peroxidation was measured as TBARS generation as described in Materials and methods. TBARS generation was evaluated in Syn and DRMs from adult and aged animals after exposure to 50 μM $FeSO_4$ or to the control condition (ultrapure water) for 1 h. Results are expressed as Abs 535 nm/μmol PLs. Asterisks indicate significant differences between adults and aged animals (**p<0.01; *p<0.05).

4. Discussion

Synaptic signaling plays important roles in modulating the activity of neuronal circuits and neuronal survival. In this work, we investigate the regulatory mechanisms involved in DAG generation elicited by PLD activation under synaptic oxidative stress.

Previous results from our laboratory have demonstrated that oxidative stress induced by free iron stimulates the generation of the lipid messenger DAG from PC in Syn from adult and aged rats. Moreover, the increase in phosphatidylethanol (PEtOH) levels in synaptosomes exposed to free iron corroborated the activation of PLDs [11]. In this connection, PLD activity has been shown to be activated by a fragment of amyloid beta (Aβ 25–35) in neuronal LA-N-2 cells and it has been also shown that Aβ 1–40 increases PLD activity in hippocampal slices in a time course that resembles LDH release and neurotoxicity [30]. An increased PLD activity has also been found in *post-mortem* brains from Alzheimer's patients [31,32].

Since both PLD isoforms are able to transphosphatidylate and generate phosphatidylalcohols, PLD1 and PLD2 activities are not distinguishable by PEtOH measurement. We therefore used two novel isoform-specific inhibitors for PLD1 (EVJ) and PLD2 (APV) in order to further study the participation of each isoform in DAG generation induced by free iron. These two novel inhibitors are a very useful and promising tool to discriminate between PLD1 and PLD2 activities in cellular-free systems as synaptosomes, in which other strategies, such as interference RNA, cannot be used [33,34]. The use of EtOH, EVJ (PLD1 inhibitor) and APV (PLD2 inhibitor) demonstrated that under control conditions basal PLD2 is responsible for DAG formation in CC Syn. This finding is consistent with the higher basal activity of PLD2 compared to that of PLD1 observed in a wide variety of tissues [6,35]. However, in Syn exposed to oxidative stress the sum of the effect of both inhibitors is coincident with the decrease observed in the

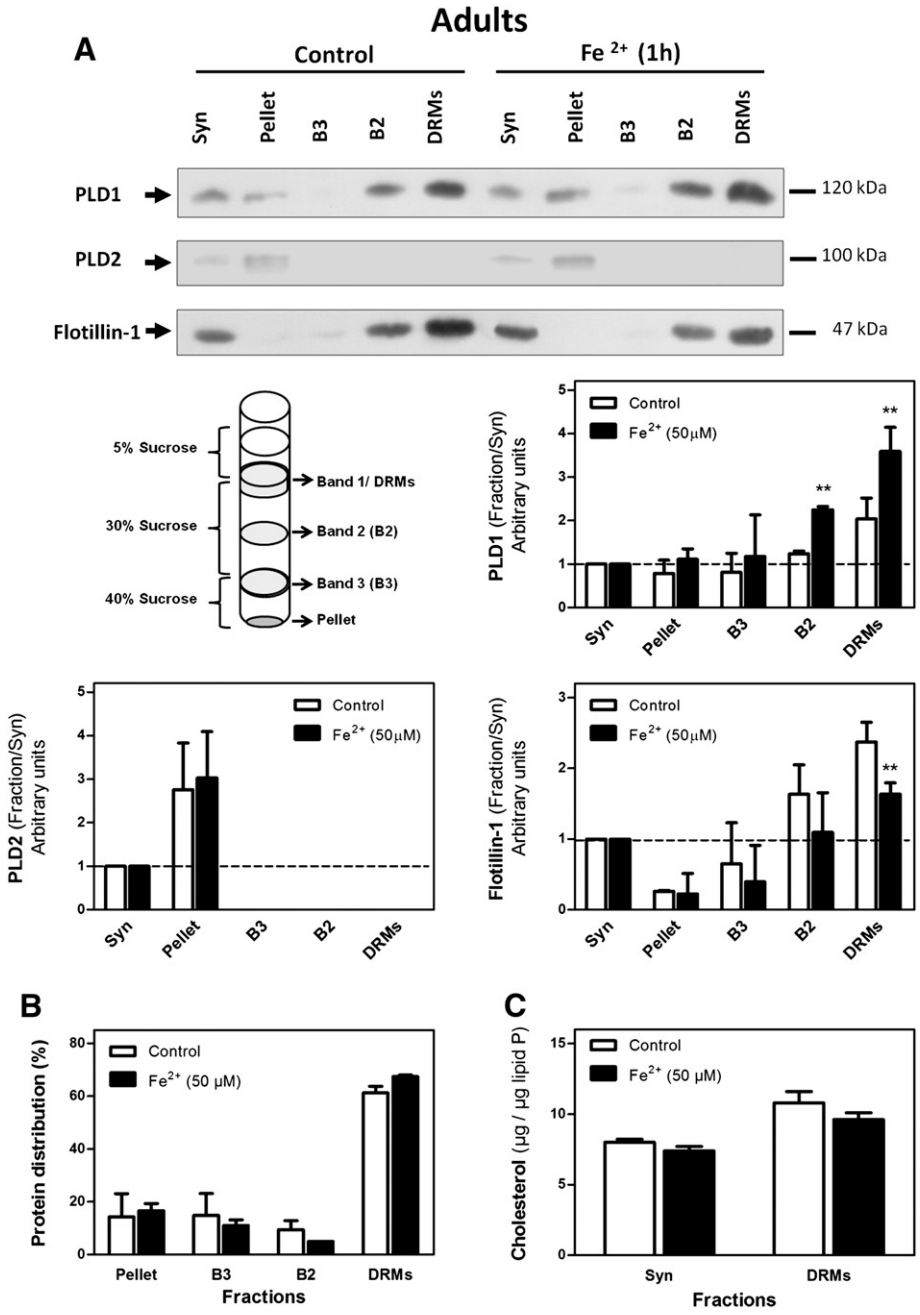

Fig. 8. A) PLD1, PLD2 and Flotillin-1 distribution in the sucrose gradient used for DRMs isolation. DRMs and the subsequent fractions of the gradient (B2, B3 and Pellet) were isolated from Syn from adult rats exposed to 50 μM $FeSO_4$ or to the control condition (ultrapure water) for 1 h as described in Materials and methods. The presence of PLD1, PLD2 and Flotillin-1 in the different fractions was determined by WB as described in Fig. 3. Numbers to the right indicate molecular weights. The bar graph shows the densitometry values of protein content in the fraction with respect to synaptosomal content. Results expressed as arbitrary units. Asterisks indicate significant differences with respect to control condition (**$p<0.01$). B) Total protein distribution among the different fractions of the sucrose gradient. Total protein content in the different fractions was measured using the DC protein assay kit from Bio-Rad. Results are expressed as percentage. C) Cholesterol content in Syn and DRMs. Total cholesterol was measured in Syn and DRMs using an enzymatic method described in Materials and methods. Results are expressed as μg cholesterol/μg lipid P.

presence of 2% EtOH, thus demonstrating that the increase in DAG generation triggered by iron-induced oxidative stress is due to the activation of both PLD isoforms. In previous research from our laboratory, a similar decrease in DAG levels when Syn were incubated with 2% EtOH or DL-propranolol (used as LPP inhibitors) was observed when measuring PC hydrolysis, thus confirming the contribution of PLD/LPP pathway and the effective conversion of PA into PEth [19].

In CC Syn from adult rats, the activation of ERK1/2, PKCα/βII and PKD1 induced by oxidative stress is regulated by DAG produced by PLD1 and PLD2 activities. In contrast, in Syn from aged animals, DAG formation from PC is an event regulated by PKCs and MEK under oxidative injury conditions and DAG generated by PLD activities does not participate in the regulation of ERK1/2, PKCα/βII and PKD1.

PKD isoforms are activated in response to numerous stimuli including reactive oxygen species [36]. Moreover, PKD1 has been identified as a mitochondrial sensor for oxidative stress which regulates a radical-sensing signaling pathway to mediate cellular detoxification and survival [37]. PKD1 gains full activity after phosphorylation by novel PKC isoforms (PKCε, PKCθ, PKCπ, and PKCδ) although only PKCδ regulates PKD1 activity in response to oxidative stress [38]. In line with this, we found that PKD1 activation by oxidative stress in CC synaptic endings is consistent with PKCδ activation.

On the other hand, it is well known that aging renders the brain increasingly susceptible to oxidative stress [9,39]. Our results demonstrate that aging induces significant changes in the modulation of DAG generating pathways from PC and in the regulation of the above-mentioned signaling pathways in response to oxidative insult.

There is no general consensus on the crosstalk between PLD and PKC during oxidative injury although most evidences point to PKC-dependent PLD activation in the presence of Aβ or H_2O_2 [32,40]. This is similar to our findings in aged animals. However, in adults, our results suggest a differential role for PLDs on account of the fact that they modulate and regulate PKC and ERK activation under oxidative injury conditions.

ERK1/2 signaling is known to play key roles in synaptic plasticity and neuronal survival [41] and, together with other mitogen-activated protein kinases (MAPKs), such as p38 and Jun kinase (JNK), it has been involved in the pathogenesis of neurodegenerative diseases such as AD and PD. It has thus been postulated that the balance between ERK and JNK activation is a key factor in determining survival [42]. The present study provides, to our knowledge, the first line of evidence of an age-dependent differential crosstalk between PLD and ERK in the synaptic ending.

Iron-induced oxidative injury was observed to significantly reduce glutamate and GABA uptake in Syn from adult animals. Our results suggest that PLD2 and MEK/ERK pathway may counteract the deleterious effect of iron on GLT because the inhibition of these pathways reduced even more glutamate uptake. The oxidative injury also reduced glutamate uptake in Syn from aged rats and PLD2 seemed to exert the same protective role in GLT as in adult Syn. In contrast, PLD1 and some PKC seemed to negatively affect GLT function under oxidative stress conditions on account of the fact that the inhibition of these pathways restored the uptake of glutamate to the levels observed under the control conditions. This finding suggests, for the first time, a role played by PLDs in the regulation of glutamate transporters in the synaptic endings exposed to oxidative injury.

Intriguingly, none of the signaling pathways studied (PLD1, PLD2, PKC and MEK/ERK) seem to be involved in the impairment of GABA uptake induced by oxidative injury in adult Syn. In spite of the fact that GABA is a significant transmitter, little is known about the GABA system during aging [43]. Our results show that GABA uptake is severely affected in CC Syn from aged rats with respect to adults and that the uptake of this neurotransmitter was not modulated by PLDs, PKCs or MEK/ERK pathway. In line with this, previous reports demonstrated that presynaptical alterations in the GABA system are correlated with aging in the frontal cortex of the human brain [43].

On the other hand, there is no general agreement about where PLD1 and PLD2 are localized in cells due to differences in cell type and methodology [1]. We have previously demonstrated a differential localization of DAG generating pathways from PC in DRMs and Syn from adult and aged rats. Whereas PLD1 and PC-PLC were found to be concentrated in DRMs, PLD2 was excluded from this fraction [19]. Furthermore, in the membrane raft fraction, DAG formation did not decrease in the presence of EtOH, thus indicating that no transphosphatidylation activity was detected in DRMs even though PLD1 was concentrated in this fraction [19]. The association of PLD1 with caveolin has been described as an inhibitory mechanism for enzyme activity [44]. Moreover, the lack of cofactors in membrane rafts such as the positive regulators of PLD activity, ARF, RhoA and cdc42, could be another reason for non detectable PLD1 activity in these specialized domains. Preliminary data from our laboratory demonstrates the absence of RhoA in DRMs (unpublished results). In the present work we further studied the effect of iron exposure on DAG generation in the DRM fraction. In membrane rafts from adult rats DAG generation from PC was not increased by iron treatment, neither in the presence nor in the absence of EtOH, demonstrating that oxidative stress does not increase DAG generation in the membrane raft fraction in spite of the enrichment in PLD1. In addition, oxidative stress was observed not to increase lipid peroxidation levels in the DRM fraction but to induce an enhanced localization of PLD1 in these microdomains.

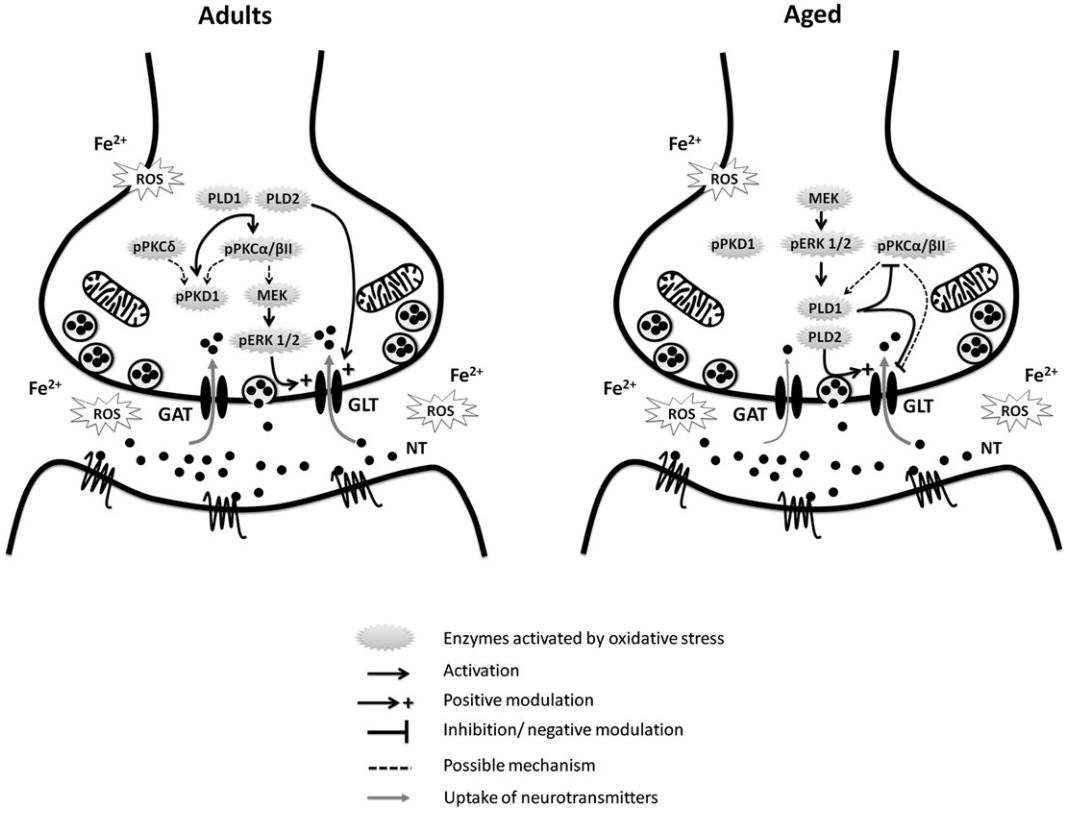

Fig. 9. Schematic view of signaling events elicited by oxidative stress and their regulation in Syn from adult and aged rats.

Localization of PLD2 was not modified and the fact that TBARs were not increased in DRMs is in accordance with the more saturated fatty acid composition previously reported about this fraction [19]. Likewise, PLD activity was not affected by oxidative stress in DRM obtained from aged animals (data not shown). These results are in agreement with the unchanged levels of lipid peroxides. It thus seems that the activation of PLDs during oxidative stress could be triggered by the increase in lipid peroxides in synaptic membranes, as it has been previously shown [45,46]. Based on these findings, it could be assumed that PLD1 localization in membrane rafts is a mechanism to either prevent or close DAG signaling elicited by oxidative injury.

Taken together, findings from our study lead us to conclude that both PLD isoforms (PLD1 and PLD2) differentially participate in the iron-induced generation of the lipid messenger DAG in rat CC Syn from adult and aged animals. Furthermore, whereas a strong correlation between PLD activities and PKD1, ERK1/2 and PKCα/βII downstream modulation was observed in adult animals, this effect was not observed in aged animals. In contrast, in senile Syn, DAG generated by PLDs was regulated by PKCs and ERK (Fig. 9). In addition, PLD2 and MEK/ERK pathway appear to play a protective role preventing, in part, the deleterious effect of iron on GLT in adult animals. In aged animals, PLD2 seems to have the same effect on the transporter activity while ERK1/2 role seems to be impaired and PLD1 exerts a negative modulation in GLT activity (Fig. 9). It can also be concluded that the age-related changes reported in the present study are likely to participate in the decline of cognitive functions and neuronal plasticity and survival in the elderly.

Abbreviations

Aβ	amyloid-β
AD	Alzheimer's disease
ALD	amyotrophic lateral sclerosis
CC	cerebral cortex
DAG	diacylglycerol
DOG	1,2-dioctanoyl-sn-glycerol
DPPC	dipalmitoylphosphatidylcholine
DRMs	detergent resistant membranes
DTT	dithiothreitol
GABA	gamma aminobutyric acid
GAT	GABA transporter
GLT	glutamate transporter
HD	Huntington's disease
ERK	extracellular signal-regulated kinase
EtOH	ethanol
HRP	horseradish peroxidise
lipid P	lipid phosphorus
JNK	Jun kinase
LPP	lipid phosphate phosphatases
MAPKs	Mitogen-activated protein kinases
PA	phosphatidic acid
PC	phosphatidylcholine
PC-PLC	phosphatidylcholine specific-phospholipase C
PD	Parkinson's disease
PEtOH	phosphatidylethanol
PIP_2	phosphatidylinositol bisphosphate
PKC	protein kinase C
PKD	protein kinase D
PLD	phospholipase D
PLs	phospholipids
PMSF	phenylmethylsulfonilfluoride
PUFA	polyunsaturated fatty acids
PVDF	polyvinylidene fluoride
RNS	reactive nitrogen species
ROS	reactive oxygen species
SDS	sodium dodecyl sulfate
SDS-PAGE	sodium dodecyl sulfate-polyacrylamide gel electrophoresis
Syn	synaptosomes
TBARS	thiobarbituric acid reactive substances
TBM	tris buffer medium
TLC	thin-layer chromatography
WB	western blot

Authors contribution

Melina V. Mateos and Gabriela A. Salvador designed the experiments and prepared the manuscript. Melina V. Mateos performed the experiments. Gabriela A. Salvador and Norma M. Giusto supervised the project.

Funding

This work was supported by grants from the Universidad Nacional del Sur, the Consejo Nacional de Investigaciones Científicas y Técnicas (PIP-CONICET) and the Agencia Nacional de Promoción Científica y Tecnológica (ANPCYT). Authors are research members of CONICET.

Acknowledgements

Authors want to thank Dr. Xosé Bustelo from the "Centro de Investigación del Cáncer" (CIC), University of Salamanca, Spain, for kindly providing the anti-PKCs, anti-PKD1 and anti-ERK antibodies. Authors are grateful to translator Viviana Soler for her technical assistance in controlling the use of the English language.

References

[1] J.H. Exton, Regulation of phospholipase D, FEBS Lett. 531 (2002) 58–61.
[2] D.A. Foster, L. Xu, Phospholipase D in cell proliferation and cancer, Mol. Cancer Res. 1 (2003) 789–800.
[3] W.C. Colley, T.C. Sung, R. Roll, J. Jenco, S.M. Hammond, Y. Altshuller, D. Bar-Sagi, A.J. Morris, M.A. Frohman, Phospholipase D2, a distinct phospholipase D isoform with novel regulatory properties that provokes cytoskeletal reorganization, Curr. Biol. 7 (1997) 191–201.
[4] S.M. Hammond, Y.M. Altshuller, T.C. Sung, S.A. Rudge, K. Rose, J. Engebrecht, A.J. Morris, M.A. Frohman, Human ADP-ribosylation factor-activated phosphatidylcholine-specific phospholipase D defines a new and highly conserved gene family, J. Biol. Chem. 270 (1995) 29640–29643.
[5] S.M. Hammond, J.M. Jenco, S. Nakashima, K. Cadwallader, Q. Gu, S. Cook, Y. Nozawa, G.D. Prestwich, M.A. Frohman, A.J. Morris, Characterization of two alternately spliced forms of phospholipase D1. Activation of the purified enzymes by phosphatidylinositol 4,5-bisphosphate, ADP-ribosylation factor, and Rho family monomeric GTP-binding proteins and protein kinase C-alpha, J. Biol. Chem. 272 (1997) 3860–3868.
[6] J. Klein, Functions and pathophysiological roles of phospholipase D in the brain, J. Neurochem. 94 (2005) 1473–1487.
[7] Z.H. Guo, M.P. Mattson, Neurotrophic factors protect cortical synaptic terminals against amyloid and oxidative stress-induced impairment of glucose transport, glutamate transport and mitochondrial function, Cereb. Cortex 10 (2000) 50–57.
[8] B. Halliwell, Role of free radicals in the neurodegenerative diseases: therapeutic implications for antioxidant treatment, Drugs Aging 18 (2001) 685–716.
[9] G.A. Salvador, R.M. Uranga, N.M. Giusto, Iron and mechanisms of neurotoxicity, Int. J. Alzheimers Dis. 2011 (2010) 720658.
[10] J.N. Keller, R.J. Mark, A.J. Bruce, E. Blanc, J.D. Rothstein, K. Uchida, G. Waeg, M.P. Mattson, 4-Hydroxynonenal, an aldehydic product of membrane lipid peroxidation, impairs glutamate transport and mitochondrial function in synaptosomes, Neuroscience 80 (1997) 685–696.
[11] M.V. Mateos, R.M. Uranga, G.A. Salvador, N.M. Giusto, Activation of phosphatidylcholine signalling during oxidative stress in synaptic endings, Neurochem. Int. 53 (2008) 199–206.
[12] R.M. Uranga, M.V. Mateos, N.M. Giusto, G.A. Salvador, Activation of phosphoinositide-3 kinase/Akt pathway by $FeSO_4$ in rat cerebral cortex synaptic endings, J. Neurosci. Res. 85 (2007) 2924–2932.
[13] D. Berg, M.B. Youdim, Role of iron in neurodegenerative disorders, Top. Magn. Reson. Imaging 17 (2006) 5–17.
[14] L.R. Freeman, J.N. Keller, Oxidative stress and cerebral endothelial cells: regulation of the blood–brain-barrier and antioxidant based interventions, Biochim. Biophys. Acta 1822 (2011) 822–829.
[15] W.Y. Ong, A.A. Farooqui, Iron, neuroinflammation, and Alzheimer's disease, J. Alzheimers Dis. 8 (2005) 183–200.
[16] R.B. Petersen, A. Nunomura, H.G. Lee, G. Casadesus, G. Perry, M.A. Smith, X. Zhu, Signal transduction cascades associated with oxidative stress in Alzheimer's disease, J. Alzheimers Dis. 11 (2007) 143–152.

[17] Y. Banno, K. Ohguchi, N. Matsumoto, M. Koda, M. Ueda, A. Hara, I. Dikic, Y. Nozawa, Implication of phospholipase D2 in oxidant-induced phosphoinositide 3-kinase signaling via Pyk2 activation in PC12 cells, J. Biol. Chem. 280 (2005) 16319–16324.
[18] P.S. Tappia, M.R. Dent, N.S. Dhalla, Oxidative stress and redox regulation of phospholipase D in myocardial disease, Free Radic. Biol. Med. 41 (2006) 349–361.
[19] M.V. Mateos, G.A. Salvador, N.M. Giusto, Selective localization of phosphatidylcholine-derived signaling in detergent-resistant membranes from synaptic endings, Biochim. Biophys. Acta 1798 (2010) 624–636.
[20] C.W. Cotman, Isolation of synaptosomal and synaptic plasma membrane fractions, Methods Enzymol. 31 (1974) 445–452.
[21] O.H. Lowry, N.J. Rosebrough, A.L. Farr, R.J. Randall, Protein measurement with the Folin phenol reagent, J. Biol. Chem. 193 (1951) 265–275.
[22] D.A. Brown, J.K. Rose, Sorting of GPI-anchored proteins to glycolipid-enriched membrane subdomains during transport to the apical cell surface, Cell 68 (1992) 533–544.
[23] G. Rouser, S. Fkeischer, A. Yamamoto, Two dimensional then layer chromatographic separation of polar lipids and determination of phospholipids by phosphorus analysis of spots, Lipids 5 (1970) 494–496.
[24] A. Adamczyk, A. Kazmierczak, J.B. Strosznajder, Alpha-synuclein and its neurotoxic fragment inhibit dopamine uptake into rat striatal synaptosomes. Relationship to nitric oxide, Neurochem. Int. 49 (2006) 407–412.
[25] U.K. Laemmli, Cleavage of structural proteins during the assembly of the head of bacteriophage T4, Nature 227 (1970) 680–685.
[26] A.I. Duarte, M.S. Santos, R. Seica, C.R. Oliveira, Oxidative stress affects synaptosomal gamma-aminobutyric acid and glutamate transport in diabetic rats: the role of insulin, Diabetes 53 (2004) 2110–2116.
[27] J.H. Jang, Y.J. Surh, Beta-amyloid-induced apoptosis is associated with cyclooxygenase-2 up-regulation via the mitogen-activated protein kinase-NF-kappaB signaling pathway, Free Radic. Biol. Med. 38 (2005) 1604–1613.
[28] J.B. Helms, C. Zurzolo, Lipids as targeting signals: lipid rafts and intracellular trafficking, Traffic 5 (2004) 247–254.
[29] L.J. Pike, Rafts defined: a report on the keystone symposium on lipid rafts and cell function, J. Lipid Res. 47 (2006) 1597–1598.
[30] D.A. Cox, M.L. Cohen, Amyloid beta-induced neurotoxicity is associated with phospholipase D activation in cultured rat hippocampal cells, Neurosci. Lett. 229 (1997) 37–40.
[31] J.N. Kanfer, I.N. Singh, J.W. Pettegrew, D.G. McCartney, G. Sorrentino, Phospholipid metabolism in Alzheimer's disease and in a human cholinergic cell, J. Lipid Mediat. Cell Signal. 14 (1996) 361–363.
[32] I.N. Singh, G. Sorrentino, J.N. Kanfer, Activation of LA-N-2 cell phospholipase D by amyloid beta protein (25–35), Neurochem. Res. 23 (1998) 1225–1232.
[33] R. Lavieri, S.A. Scott, J.A. Lewis, P.E. Selvy, M.D. Armstrong, B.H. Alex, C.W. Lindsley, Design and synthesis of isoform-selective phospholipase D (PLD) inhibitors. Part II. Identification of the 1,3,8-triazaspiro[4,5]decan-4-one privileged structure that engenders PLD2 selectivity, Bioorg. Med. Chem. Lett. 19 (2009) 2240–2243.
[34] J.A. Lewis, S.A. Scott, R. Lavieri, J.R. Buck, P.E. Selvy, S.L. Stoops, M.D. Armstrong, H.A. Brown, C.W. Lindsley, Design and synthesis of isoform-selective phospholipase D (PLD) inhibitors. Part I: impact of alternative halogenated privileged structures for PLD1 specificity, Bioorg. Med. Chem. Lett. 19 (2009) 1916–1920.
[35] T. Hu, J.H. Exton, Mechanisms of regulation of phospholipase D1 by protein kinase C alpha, J. Biol. Chem. 278 (2003) 2348–2355.
[36] R.T. Waldron, E. Rozengurt, Oxidative stress induces protein kinase D activation in intact cells. Involvement of Src and dependence on protein kinase C, J. Biol. Chem. 275 (2000) 17114–17121.
[37] P. Storz, Mitochondrial ROS–radical detoxification, mediated by protein kinase D, Trends Cell Biol. 17 (2007) 13–18.
[38] H. Doppler, P. Storz, A novel tyrosine phosphorylation site in protein kinase D contributes to oxidative stress-mediated activation, J. Biol. Chem. 282 (2007) 31873–31881.
[39] M.D. Ledesma, M.G. Martin, C.G. Dotti, Lipid changes in the aged brain: effect on synaptic function and neuronal survival, Prog. Lipid Res. 51 (2012) 23–35.
[40] J. Kim, G. Min, Y.S. Bae, D.S. Min, Phospholipase D is involved in oxidative stress-induced migration of vascular smooth muscle cells via tyrosine phosphorylation and protein kinase C, Exp. Mol. Med. 36 (2004) 103–109.
[41] Y. Dwivedi, H.S. Rizavi, H. Zhang, R.C. Roberts, R.R. Conley, G.N. Pandey, Aberrant extracellular signal-regulated kinase (ERK)1/2 signalling in suicide brain: role of ERK kinase 1 (MEK1), Int. J. Neuropsychopharmacol. 12 (2009) 1337–1354.
[42] E.K. Kim, E.J. Choi, Pathological roles of MAPK signaling pathways in human diseases, Biochim. Biophys. Acta 1802 (2010) 396–405.
[43] I. Sundman-Eriksson, P. Allard, Age-correlated decline in [^{3}H]tiagabine binding to GAT-1 in human frontal cortex, Aging Clin. Exp. Res. 18 (2006) 257–260.
[44] J.H. Kim, J.M. Han, S. Lee, Y. Kim, T.G. Lee, J.B. Park, S.D. Lee, P.G. Suh, S.H. Ryu, Phospholipase D1 in caveolae: regulation by protein kinase C alpha and caveolin-1, Biochemistry 38 (1999) 3763–3769.
[45] V. Natarajan, W.M. Scribner, M.M. Taher, 4-Hydroxynonenal, a metabolite of lipid peroxidation, activates phospholipase D in vascular endothelial cells, Free Radic. Biol. Med. 15 (1993) 365–375.
[46] V. Natarajan, M.M. Taher, B. Roehm, N.L. Parinandi, H.H. Schmid, Z. Kiss, J.G. Garcia, Activation of endothelial cell phospholipase D by hydrogen peroxide and fatty acid hydroperoxide, J. Biol. Chem. 268 (1993) 930–937.